9
Baroclinic Rossby Waves and Cyclogenesis

Abstract of a landmark article on the theory of cyclogenesis

By obtaining complete solutions, satisfying all relevant simultaneous differential equations and boundary conditions, representing small disturbances of simple states of steady baroclinic large-scale atmospheric motion it is shown that these simple states of motion are almost invariably unstable. An arbitrary disturbance (corresponding to some inhomogeneity of an actual system) may be regarded as analysed into "components" of a certain simple type, some of which grow exponentially with time. In all the cases examined there exists one particular component that grows faster than any other. It is shown how, by a process analogous to "natural selection", this component becomes dominant in that almost any disturbance tends eventually to a definite size, structure and growthrate (and to a characteristic life-history after the disturbance has ceased to be "small"), which depends only on the broad characteristics of the initial (unperturbed) system. The characteristic disturbances (forms of breakdown) of certain types of initial system (approximating to those in practice) are identified as the ideal forms of the observed cyclone waves and long waves of middle and high latitudes.
E.T. Eady (1949), "Long waves and cyclone waves" (**Tellus**, 1, 33-52)

http://www.staff.science.uu.nl/~delde102/AtmosphericDynamics.htm

9.1 Introduction

The formation or genesis of cyclones (**cyclogenesis**) occurs most frequently in zones which exhibit strong low level horizontal temperature gradients. These so-called **baroclinic zones** are encountered most frequently in the winter in middle latitudes. In section 9.2 a two-level quasi-geostrophic model of the atmosphere is introduced, which is the minimum-complexity model, which permits the existence baroclinic Rossby waves, which are Rossby waves which have a non-constant or non-homogeneous vertical structure. Linear analysis of the stability of a zonal baroclinic zone, characterised by a meridional temperature gradient, in thermal wind balance, in this two-level model, reveals that baroclinic Rossby waves may become unstable and grow exponentially in time. The structure and scale of these waves is very similar to the cyclone waves which are observed in middle latitudes in reality. Potential vorticity, which is obviously also a useful concept in this context, will return into the discussion at the end of this chapter and in subsequent chapters. This reflects the two somewhat different viewpoints on mid-latitude atmospheric dynamics that presently exist side by side.

Box 9.1 Primitive equations in pressure coordinates

With the ideal gas law, $p=\rho RT$, the hydrostatic equation, $\partial p=-\rho g\partial z$, can be written as

$$\boxed{\frac{\partial \Phi}{\partial p} = -\frac{RT}{p}}\ , \qquad (1)$$

where the "**geopotential**" is

$$\boxed{\Phi \equiv gz}\ . \qquad (2)$$

Integration of (1) in the vertical yields the **hypsometric equation**:

$$z_T \equiv z_2 - z_1 = \frac{R}{g}\int_{p_2}^{p_1} T d(\ln p)\ , \qquad (3)$$

The quantity, z_T, is the **thickness** of the atmospheric layer between the pressure surfaces p_2 and p_1.

Defining the layer mean temperature as

$$\langle T\rangle \equiv \int_{p_2}^{p_1} T d(\ln p)\left[\int_{p_2}^{p_1} d(\ln p)\right]^{-1}\ , \qquad (4)$$

we obtain

$$z_T = \frac{R}{g}\langle T\rangle \ln\frac{p_1}{p_2}\ . \qquad (5a)$$

Thus, the thickness of a layer bounded by isobaric surfaces is proportional to the mean

temperature of the layer. We can also write this equation as

$$z_T \equiv H \ln \frac{p_1}{p_2} \ . \tag{5b}$$

with the layer mean scale height defined as

$$H \equiv \frac{R\langle T \rangle}{g} \ . \tag{6}$$

The thermodynamic energy equation (1.195) is written in pressure coordinates as follows.

$$\frac{\partial T}{\partial t} + u\left(\frac{\partial T}{\partial x}\right)_p + v\left(\frac{\partial T}{\partial y}\right)_p + \omega \frac{\partial T}{\partial p} - \frac{\alpha\omega}{c_p} = \frac{J}{c_p} \ , \tag{7}$$

where the differentiation with respect to x and y is done at constant pressure, and where c_p is the specific heat at constant pressure (c_p-c_v=R).

Eq. 7 is rewritten as

$$\boxed{\frac{\partial T}{\partial t} + u\left(\frac{\partial T}{\partial x}\right)_p + v\left(\frac{\partial T}{\partial y}\right)_p - S_p\omega = \frac{J}{c_p}}, \tag{8}$$

where, with the aid of eqs. 1.10b and 1.21, we have

$$S_p \equiv \frac{RT}{c_p p} - \frac{\partial T}{\partial p} = -\frac{T}{\theta}\frac{\partial \theta}{\partial p} \ , \tag{9}$$

which is the **static stability parameter for the isobaric system**.

With **pressure** as a vertical coordinate, the horizontal components of the momentum are (see 1.191a,b) are

$$\frac{du}{dt} - \frac{uv\tan\phi}{a} = -\left(\frac{\partial \Phi}{\partial x}\right)_p + fv + F_x \ , \tag{10a}$$

$$\frac{dv}{dt} + \frac{u^2\tan\phi}{a} = -\left(\frac{\partial \Phi}{\partial y}\right)_p - fu + F_y \ . \tag{10b}$$

with

$$\boxed{\frac{d}{dt} = \frac{\partial}{\partial t} + u\left(\frac{\partial}{\partial x}\right)_p + v\left(\frac{\partial}{\partial y}\right)_p + \omega\frac{\partial}{\partial p}} \ . \tag{11}$$

If applied to large scale motion systems in **mid-latitudes**, eqs. 10a,b are frequently simplified to (**Box 1.6**)

$$\boxed{\frac{du}{dt} = -\frac{\partial \Phi}{\partial x} + fv} \tag{12a}$$

$$\boxed{\frac{dv}{dt} = -\frac{\partial \Phi}{\partial y} - fu} \tag{12b}$$

The continuity equation in the pressure coordinate system is (eq. 1.209)

$$-\frac{v \tan\phi}{a} + \left(\frac{\partial u}{\partial x} + \frac{\partial v}{\partial y}\right)_p + \frac{\partial \omega}{\partial p} = 0 \ , \tag{13}$$

which, when applied to mid-latitudes, is usually simplified to

$$\boxed{\left(\frac{\partial u}{\partial x} + \frac{\partial v}{\partial y}\right)_p + \frac{\partial \omega}{\partial p} = 0} \ . \tag{14}$$

The continuity equation (14), the hydrostatic relation (1), the thermodynamic equation (8) and the momentum equation (12a,b) form a closed set of equations, also referred to as the "**primitive equations**", which can be solved, given boundary conditions in space and time.

9.2 The two level model

In this section we discuss the role of the instability of thermal wind balance in accounting for the growth of mid-latitude cyclones.

The most simplified model of the atmosphere that can incorporate three-dimensional baroclinic processes has two discrete layers, bounded by surfaces numbered 0, 2 and 4, as shown in **figure 9.1**. The geostrophic wind (1.246), which in vector-notation is

$$\vec{v}_g \equiv f_0^{-1} \hat{k} \times \vec{\nabla} \Phi, \tag{9.1}$$

and the geostrophic vorticity (1.249) can be expressed respectively as

$$\boxed{\zeta_g = \frac{1}{f_0}\left(\frac{\partial^2 \Phi}{\partial x^2} + \frac{\partial^2 \Phi}{\partial y^2}\right) \equiv \frac{1}{f_0}\nabla^2 \Phi} \ . \tag{9.2}$$

It is convenient to define a **geostrophic streamfunction**, $\psi = \Phi / f_0$, so that

$$\vec{v}_g = \hat{k} \times \vec{\nabla} \psi, \ \zeta_g = \nabla^2 \psi \ . \tag{9.3}$$

Remember that $\nabla^2 \equiv \nabla_h^2$.

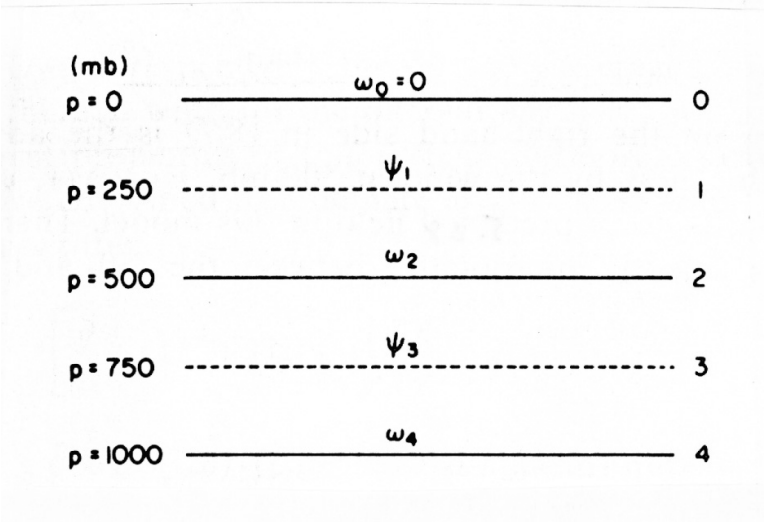

FIGURE 9.1. Arrangement of variables in the vertical direction for the two-level model (from Holton, 2004).

In terms of ψ, the quasi-geostrophic vorticity equation (1.251) becomes

$$\frac{\partial \nabla^2 \psi}{\partial t} + \vec{v}_g \cdot \vec{\nabla}\left(\nabla^2 \psi\right) + \beta \frac{\partial \psi}{\partial x} = f_0 \frac{\partial \omega}{\partial p} \tag{9.4}$$

Using the hydrostatic relation (eq. 1, **box 9.1**) and neglecting heating (J=0), the quasi-geostrophic thermodynamic equation (1.316) can be written as

$$\frac{\partial}{\partial t}\left(\frac{\partial \psi}{\partial p}\right) + \vec{v}_g \cdot \vec{\nabla}\left(\frac{\partial \psi}{\partial p}\right) = -\frac{\sigma}{f_0}\omega \tag{9.5}$$

We now "apply" (9.35) at levels 1 and 3. To do this we must estimate the divergence term at these levels using finite difference approximations to the vertical derivatives:

$$\left(\frac{\partial \omega}{\partial p}\right)_1 \approx \frac{\omega_2 - \omega_0}{\delta p} \ , \left(\frac{\partial \omega}{\partial p}\right)_3 \approx \frac{\omega_4 - \omega_2}{\delta p} \ . \tag{9.6}$$

Here δp is the pressure interval between the levels 0 and 2, and 2 and 4. Subscripts indicate the vertical level for each dependent variable.

The resulting vorticity equations are

$$\frac{\partial \nabla^2 \psi_1}{\partial t} + \vec{v}_1 \cdot \vec{\nabla}\left(\nabla^2 \psi_1\right) + \beta \frac{\partial \psi_1}{\partial x} = \frac{f_0}{\delta p}\omega_2 \ , \tag{9.7}$$

$$\frac{\partial \nabla^2 \psi_3}{\partial t} + \vec{v}_3 \cdot \vec{\nabla}\left(\nabla^2 \psi_3\right) + \beta \frac{\partial \psi_3}{\partial x} = -\frac{f_0}{\delta p}\omega_2 \ . \tag{9.8}$$

here we have used the fact that ω_0=0 and assumed that ω_4=0.

We next write the thermodynamic energy equation (9.5) at level 2. Here we must evaluate $\partial\psi/\partial p$ using the approximate formula

$$\left(\frac{\partial\psi}{\partial p}\right)_2 \approx \frac{\psi_3 - \psi_1}{\delta p} \ . \tag{9.9}$$

This yields

$$\frac{\partial}{\partial t}(\psi_1 - \psi_3) = -\vec{v}_2 \cdot \vec{\nabla}(\psi_1 - \psi_3) + \frac{\sigma\delta p}{f_0}\omega_2 \ . \tag{9.10}$$

The first term on the r.h.s. in (9.10) represents advection of the 250-750 hPa thickness by the wind at 500 hPa. However, the 500 hPa streamfunction, ψ_2, is not a predicted field in this model. Therefore, ψ_2 must be obtained by linearly interpolating between 250 hPa and 750 hPa as follows:

$$\psi_2 \approx \frac{(\psi_1 - \psi_3)}{2} \ . \tag{9.11}$$

If this formula is used, (9.7), (9.8) and (9.10) become a closed set of prediction equations in the variables ψ_1, ψ_3 and ω_2.

9.3 Linear analysis: Rossby waves and baroclinic instability

In order to simplify the analysis as much as possible we assume that the streamfunctions, ψ_1 and ψ_3, can be expressed as follows

$$\begin{aligned} \psi_1 &= -U_1 y + \psi_1'(x,y,t), \\ \psi_3 &= -U_3 y + \psi_3'(x,y,t), \\ \omega_2 &\approx \omega_2'(x,y,t). \end{aligned} \tag{9.12}$$

The "background" geostrophic zonal velocities at levels 1 and 3 are constants with the values U_1 and U_3, respectively.

Substituting (9.12) into (9.7-8) and (9.10) and linearising yields the perturbation equations,

$$\left(\frac{\partial}{\partial t} + U_1\frac{\partial}{\partial x}\right)\nabla_h^2\psi_1' + \beta\frac{\partial\psi_1'}{\partial x} = \frac{f_0}{\delta p}\omega_2', \tag{9.13}$$

$$\left(\frac{\partial}{\partial t} + U_3\frac{\partial}{\partial x}\right)\nabla_h^2\psi_3' + \beta\frac{\partial\psi_3'}{\partial x} = \frac{-f_0}{\delta p}\omega_2', \tag{9.14}$$

$$\left(\frac{\partial}{\partial t} + U_m\frac{\partial}{\partial x}\right)(\psi_1' - \psi_3') - U_T\frac{\partial}{\partial x}(\psi_1' + \psi_3') = \frac{\sigma\delta p}{f_0}\omega_2', \tag{9.15}$$

with

$$\nabla_h^2 \equiv \frac{\partial^2}{\partial x^2} + \frac{\partial^2}{\partial y^2}.$$

We have linearly interpolated to express v_2 in terms of ψ_1 and ψ_3, i.e.

$$v_2 = v'_2 = \frac{1}{2}(v'_1 + v'_3) = \frac{1}{2}\frac{\partial}{\partial x}(\psi'_1 + \psi'_3),$$

and we have defined

$$U_M \equiv \frac{(U_1 + U_3)}{2} \text{ and } U_T \equiv \frac{(U_1 - U_3)}{2} \ . \tag{9.16}$$

Thus, U_M and U_T are respectively, the vertically averaged zonal wind and the mean thermal wind for the interval between levels 1 and 3.

The dynamical properties of this system are more clearly expressed if (9.13-15) are combined to eliminate ω_2'. First we write (9.13) and (9.14) as

$$\left(\frac{\partial}{\partial t} + (U_M + U_T)\frac{\partial}{\partial x}\right)\nabla_h^2\psi_1' + \beta\frac{\partial\psi_1'}{\partial x} = \frac{f_0}{\delta p}\omega_2' \quad , \tag{9.17}$$

$$\left(\frac{\partial}{\partial t} + (U_M - U_T)\frac{\partial}{\partial x}\right)\nabla_h^2\psi_3' + \beta\frac{\partial\psi_3'}{\partial x} = -\frac{f_0}{\delta p}\omega_2' \quad , \tag{9.18}$$

We now define the barotropic and baroclinic perturbations as

$$\psi_M \equiv \frac{(\psi_1 + \psi_3)}{2} \text{ and } \psi_T \equiv \frac{(\psi_1 - \psi_3)}{2} \ . \tag{9.19}$$

Adding (9.17) and (9.18) and using the definition in (9.19) yields

$$\left(\frac{\partial}{\partial t} + U_M\frac{\partial}{\partial x}\right)\nabla_h^2\psi_M + \beta\frac{\partial\psi_M}{\partial x} + U_T\frac{\partial}{\partial x}\nabla_h^2\psi_T = 0 \quad , \tag{9.20}$$

whereas subtracting (9.18) from (9.17) and combining with (9.15) to eliminate ω_2' yields

$$\left(\frac{\partial}{\partial t} + U_M\frac{\partial}{\partial x}\right)\left(\nabla_h^2\psi_T - 2\lambda^2\psi_T\right) + \beta\frac{\partial\psi_T}{\partial x} + U_T\frac{\partial}{\partial x}\left(\nabla_h^2\psi_M + 2\lambda^2\psi_M\right) = 0 \tag{9.21}$$

where

$$\boxed{\lambda^2 \equiv \frac{f_0^2}{\sigma(\delta p)^2}} \ . \tag{9.22}$$

is the **inverse of the Rossby radius of deformation within the context of this model**. Equations (9.20) and (9.21) govern the evolution of the barotropic (vertically averaged) and baroclinic (thermal) perturbation vorticities, respectively.

We assume that wavelike solutions exist of the form

$$\psi_M = A\exp\left[i(lx+my-\omega t)\right];\ \psi_T = B\exp\left[i(lx+my-\omega t)\right]. \tag{9.23}$$

Substituting these solutions into (9.20) and (9.21) we obtain a pair of simultaneous linear algebraic equations for the coefficients A and B:

$$\left[(c_x-U_M)k^2+\beta\right]A - U_T k^2 B = 0\ , \tag{9.24}$$

$$U_T\left(k^2-2\lambda^2\right)A - \left[(c_x-U_M)\left(k^2+2\lambda^2\right)+\beta\right]B = 0\ , \tag{9.25}$$

where

$k^2 \equiv l^2 + m^2$ and $c_x \equiv \omega/l$.

Non-trivial solutions will exist only if the determinant of the coefficients of A and B is zero. Thus the phase speed c must satisfy the condition

$$k^2\left(k^2+2\lambda^2\right)(c_x-U_M)^2 + 2\beta\left(k^2+\lambda^2\right)(c_x-U_M) + \left[\beta^2 - U_T^2 k^2\left(k^2-2\lambda^2\right)\right] = 0\ , \tag{9.26}$$

The dispersion relation (9.26) yields for the phase speed

$$\boxed{c_x = U_M - \frac{\beta\left(k^2+\lambda^2\right)}{k^2\left(k^2+2\lambda^2\right)} \pm \sqrt{\delta}}\ , \tag{9.27}$$

where

$$\boxed{\delta \equiv \frac{\beta^2\lambda^4}{k^4\left(k^2+2\lambda^2\right)^2} - \frac{U_T^2\left(2\lambda^2-k^2\right)}{\left(k^2+2\lambda^2\right)}}\ , \tag{9.28}$$

Although (9.27) appears to be rather complicated, it is immediately apparent that, if δ<0, the phase speed will have an imaginary part and perturbations will amplify exponentially.

Let us consider the **special case, β=0**. In this case

$$c_x = U_M \pm U_T\left(\frac{k^2-2\lambda^2}{k^2+2\lambda^2}\right)^{1/2}\ . \tag{9.29}$$

For waves with zonal wave numbers satisfying $k^2<2\lambda^2$, (9.29) has an imaginary part. Therefore, all waves with wavelengths greater than the critical wavelength $L_c = \sqrt{2}\pi/\lambda$ will amplify. The **growth rate** of this amplification is equal to ($i\omega$). From the definition of λ (9.22) we can write

$$L_c = \frac{\pi(2\sigma)^{1/2}\delta p}{f_0}\ . \tag{9.30}$$

For typical tropospheric conditions, $(2\sigma)^{1/2}\approx 2\times10^{-3}$ $N^{-1}m^3s^{-1}$. Therefore, with δp=50000 Pa and $f_0=10^{-4}$ s^{-1} we find that L_c=3000 km, which is the typical wavelength in longitudinal direction of observed synoptic disturbances. Eq. 9.30 also reveals that the critical wavelength for **baroclinic instability** increases with the static stability.

Let us now consider the **special case, U_T=0**. In this so-called **barotropic** case (9.58) reduces to either

$$c_x = U_M - \frac{\beta}{k^2} \tag{9.31a}$$

or

$$c_x = U_M - \frac{\beta}{\left(k^2 + 2\lambda^2\right)} \tag{9.31b}$$

With a barotropic basic state current, U_M, the two-level model possessses two free (normal mode) small amplitude solutions, which represent oscillations or waves, which exist due to the β–effect. These waves are termed **Rossby waves** (see also section 1.37 and problem 5.4 in section 5.3). According to (9.31) the phase of Rossby waves propagates in westerly direction relative to the basic barotropic current. Rossby waves can be identified with the troughs and ridges that are characteristic of upper air charts of the geopotential height at, for instance 500 hPa (**figure 1.112**).

It is important to note that if we set β=0 and U_T=0 in eq. 9.28, we find that the system does not support waves. This implies that **acoustic waves, gravity waves and inertial waves have been filtered out as a solution** by making the hydrostatic approximation and the quasi-geostrophic approximation. Indeed, the principal reason for developing quasi-geostrophic theory in the 1940's was to find a system of equations, which could be integrated numerically without too much computational expense, while still retaining as much of the meteorologically interesting phenomena as possible. Meteorologically the most important and interesting waves are the Rossby waves. Sound waves (**chapter 3**) are less interesting, because they do not play a role in the formation of precipitation systems. Because of their high phase velocity and high frequency, sound waves represent a significant computational burden, if they are included in the numerical solution. Buoyancy waves (**chapter 3**) require a high spatial resolution and therefore also form a significant computational burden, while only having a significant influence on the large-scale flow through the buoyancy- or gravity wave drag effect, which is discussed in **section 3.5**.

In the general case, where all terms in (9.58) are retained, the stability criterion is most easily understood by computing the neutral curve, which connects all values of U_T and k for which δ=0, so that the flow is marginally stable. The condition δ=0 implies that

$$\frac{\beta^2\lambda^4}{k^4\left(k^2+2\lambda^2\right)} = U_T^2\left(2\lambda^2 - k^2\right), \tag{9.32}$$

This complicated relationship between U_T and k can best be displayed in a graph by solving (9.32) for $k^4/2\lambda^4$, yielding

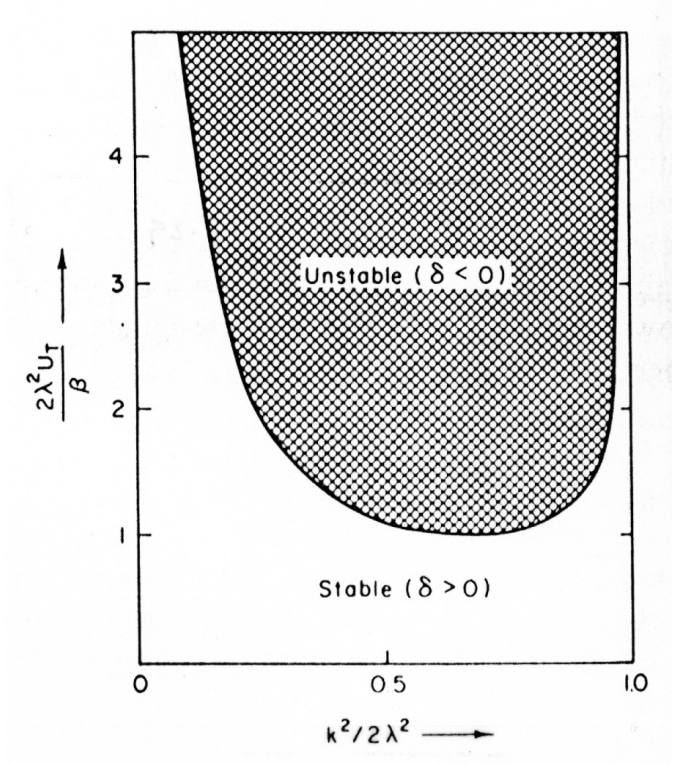

FIGURE 9.2. Neutral stability curve for the two-level baroclinic model. Source of this figure: Holton (2004) (see the list of references at the end of this chapter).

$$\frac{k^4}{2\lambda^4} = 1 \pm \left[1 - \frac{\beta^2}{4\lambda^4 U_T^2}\right]^{1/2}.$$

This equation is displayed graphically in **figure 9.2**. The nondimensional quantity $k^2/2\lambda^2$ is plotted along the horizontal axis. The nondimensional parameter $2\lambda^2 U_T/\beta$ is plotted along the vertical axis. The latter parameter is proportional to the thermal wind or meridional basic state temperature gradient. Baroclinic waves are always stable if the quantity, $k^2/(2\lambda^2)=2\pi^2\sigma(\delta p)^2/(L_x^2 f_0^2)>1$, or if

$$A_R \equiv \frac{L_x}{2\delta p} < \frac{\pi\sqrt{\sigma}}{\sqrt{2} f_0}. \qquad (9.33)$$

On the right hand side of this inequality we recognize a quantity that could be identified as the **Rossby ratio**, following the ideas of **section 1.44**. Popagating baroclinic Rossby waves are accompanied by a secondary vertical circulation (**section 1.44**). If this circulation has an aspect ratio smaller than the Rossby ratio, the amplitude of the wave will not grow due to baroclinic instability.

The neutral curve in **figure 9.2** separates the unstable region in the U_T - k plane from the stable region. The inclusion of the β-effect serves to stabilize the flow, because now unstable roots exist only for $|U_T|>\beta/(2\lambda^2)$. In addition, the minimum value of U_T required for unstable growth depends strongly on k. Thus, the β–effect stabilizes the long-wave end of the wave spectrum. Again, the flow is always stable for waves shorter than the critical wavelength,

$L_c = \pi\sqrt{2}/\lambda$. By differentiating (9.32) with respect to k and setting $dU_T/dk=0$, we find that the minimum value of U_T for which unstable waves may exist, occurs when $k^2=\sqrt{2}\lambda^2$. This wave number corresponds to the wave, which becomes unstable for the lowest value of the thermal wind. Observed gowing waves should have a wave number that lies close to this **wave number of "maximum instability"**, because, if U_T were gradually raised from zero, the flow would first become unstable for perturbations of wave number $k=2^{1/4}\lambda$. These perturbations would then amplify and in the process remove energy from the mean thermal wind, thereby decreasing U_T and stabilizing the flow. Under normal conditions of static stability, the theoretical wavelength of maximum instability is approximately 4000 km, which is of similar order of magnitude as the wavelength of growing midlatitude baroclinic waves.

The thermal wind required for marginal stability at the wavelength of maximum instability is about $U_T \approx 4$ m/s, which implies a shear of 8 m/s between 250 and 750 hPa. Comparing this with the example, which is discussed in section 9.2, we find[1] that the mean zonal wind speed on March 3, 1995 at 00 UTC within the trough or core of the jetstreak is 16 m/s at 750 hPa, and 24 m/s at 250 hPa, implying a shear of 8 m/s between these levels, which perhaps by fortune is exactly the value for marginal instability quoted above. This verifies the hypothesis that the growth of the baroclinic Rossby waves originates from "small perturbations" of a baroclinically unstable basic current.

It is, however, doubtful whether this is really the case. Numerical weather prediction models generally predict cyclogenesis with a surprising degree of accuracy many days in advance. If the time and location of cyclogenesis were really dependent on the time and location of a random infinitesimal perturbation, the performance of numerical weather prediction models would be very much worse than it actually is.

It is very likely that cyclogenesis requires finite amplitude (relatively intense) perturbations. These perturbations are in fact frequently observable as a potential vorticity anomaly. Therefore, we must not interpret the theory of baroclinic instability too literally, but more as giving valuable information about the processes causing cyclogenesis and the connection between the preferred length-scales associated with these processes and the constraints imposed on the atmosphere.

9.4 Vertical motion in small-amplitude baroclinic waves

The basic physics of a linear baroclinic wave and linear baroclinic instability can be distilled from the analysis presented in the previous section by using the omega equation, which is derived in section 1.43. The omega equation (eq. 1.359) is repeated here:

$$\nabla^2\omega + \frac{f_0^2 p}{RS_p}\frac{\partial^2\omega}{\partial p^2} = -\frac{2}{S_p}\vec{\nabla}\cdot\vec{Q}_g \qquad (9.34)$$

where the Q-vectors are defined as (see eq. 1.361):

$$\vec{Q}_g \equiv \left(Q_{g1}, Q_{g2}\right) = -\left(\frac{\partial\vec{v}_g}{\partial x}\cdot\vec{\nabla}T, \frac{\partial\vec{v}_g}{\partial y}\cdot\vec{\nabla}T\right) \qquad (9.35a)$$

[1] See the sounding made at Brest and Camborne (http://weather.uwyo.edu/upperair/sounding.html).

which can be written as,

$$Q_{g1} = -\left(\frac{\partial u_g}{\partial x}\frac{\partial T}{\partial x} + \frac{\partial v_g}{\partial x}\frac{\partial T}{\partial y}\right);\; Q_{g2} = -\left(\frac{\partial u_g}{\partial y}\frac{\partial T}{\partial x} + \frac{\partial v_g}{\partial y}\frac{\partial T}{\partial y}\right). \tag{9.35b}$$

The Q-vector, linearised around a basic state baroclinic homogeneous zonal current, as defined in (9.12), becomes (using $\partial u_g/\partial x+\partial v_g/\partial y=0$),

$$\left(Q_{g1},Q_{g2}\right) = \left(-\frac{\partial v_g}{\partial x}\frac{\partial T}{\partial y},+\frac{\partial u_g}{\partial x}\frac{\partial T}{\partial y}\right) \approx -\frac{\partial v_g}{\partial x}\frac{\partial T}{\partial y}. \tag{9.36}$$

In the Northern Hemisphere $\partial T/\partial y<0$, while in a trough of a Rossby wave we have $\partial v_g/\partial x>0$. Therefore, the Q-vector points in eastward direction in a trough and in westward direction in the ridge, where $\partial v_g/\partial x<0$. In the ridge we have $\partial v_g/\partial x<0$, which implies that the Q-vector points in westward direction. Neglecting, for simplicity, the accelerations and decelerations of the zonal current, we see that the Q-vector converges to the east of the trough and diverges to the west of the trough, which, according to the omega equation (9.34), implies upward motion to the east of the trough and downward motion to the west of the trough.

The most important frontogenetic effect, which is left in this linear analysis, is **the effect of the rotation of the isotherms** due to the shear term $\partial v_g/\partial x\partial T/\partial y$. This effect turns the isotherms from the longitudinal direction into the meridional direction. Because the atmosphere is constrained (in the theory) to remain in thermal wind balance, this requires a simultaneous turning of the thermal wind (the direction of the thermal wind vector always paprallel to the isotherms). According to eq. 1.356, which is repeated here as eq. 9.37:

$$\frac{f_0^2 p}{R}\frac{\partial u_a}{\partial p} - S_p\frac{\partial \omega}{\partial x} = 2Q_{g1} \equiv \frac{d_g}{dt}\left(\frac{\partial T}{\partial x}\right) \approx -2\frac{\partial v_g}{\partial x}\frac{\partial T}{\partial y}\;, \tag{9.37}$$

this adjustment to thermal wind balance is taken care of by an ageostrophic "circulation", (u_a, ω), in the x-p plane.

Within the framework of the two-level quasi-geostrophic model the upward motion east of the trough and west of the ridge is attended with an increase of the geostrophic relative vorticity, which is approximately equal to $v_g/\partial x$, at levels below 500 hPa, due to mass convergence. This will, in turn, enhance the frontogenetic effect of the shear term $\partial v_g/\partial x\partial T/\partial y$ and thus induce a positive feedback, i.e. instability. However, the frontogenetic effect of the ageostrophic circulation, which is proportional to $\partial\omega/\partial x\partial T/\partial p$, may counteract this feedback effect. The linear stability analysis of the balanced zonal current section, given in the previous section, indicates that this feedback is unstable when the meridional temperature gradient and associated vertical shear of the geostrophic wind (the thermal wind) exceeds a certain threshold value and when the waves have wave lengths in the oreder of several thousand km.

Let us apply the omega equation to level 2 in the two-level model (**figure 9.1**). The Q_g-vector for the two-level model can be derived simply from (9.29). We first estimate the second term on the left hand side by finite differencing in p. Using (9.6), we obtain

$$\frac{\partial^2\omega}{\partial p^2} \approx \frac{\left[\frac{\partial\omega}{\partial p}\right]_3 - \left[\frac{\partial\omega}{\partial p}\right]_1}{\delta p} \approx -\frac{2\omega_2}{(\delta p)^2}\;, \tag{9.38}$$

With eq. 1 in **Box 9.1** we have

$$T = -\frac{p}{R}\frac{\partial \Phi}{\partial p} = -\frac{f_0 p}{R}\frac{\partial \psi}{\partial p} \tag{9.39}$$

Applying this to level 2 of the two-level model we obtain

$$T_2 = \frac{f_0}{R}\left(\psi_1 - \psi_3\right). \tag{9.40}$$

Thus, the omega equation (9.34), applied to model level 2, becomes

$$\sigma\left(\nabla^2 - 2\lambda^2\right)\omega_2 = -\frac{2R}{p}\vec{\nabla}\vec{Q}_g \ , \tag{9.41}$$

Substituting (9.40) in (9.36), using (9.12) and (9.16), we obtain

$$\left(\frac{\partial^2}{\partial x^2} + \frac{\partial^2}{\partial y^2} - 2\lambda^2\right)\omega_2' = -\frac{4 f_0}{\sigma \delta p} U_T \frac{\partial}{\partial x}\frac{\partial v_2'}{\partial x} = -\frac{4 f_0}{\sigma \delta p} U_T \frac{\partial \zeta_2'}{\partial x} \ . \tag{9.42}$$

Observing that

$$\left(\frac{\partial^2}{\partial x^2} + \frac{\partial^2}{\partial y^2} - 2\lambda^2\right)\omega_2' \propto -\omega_2' \ , \tag{9.43}$$

we may write eq. 9.42, very shortly, as follows.

$$\boxed{w_2' \propto -\omega_2' \propto -U_T \frac{\partial \zeta_2'}{\partial x}} \ . \tag{9.44}$$

Thus, **sinking (rising) motion is associated with (or "induced" by) negative (positive) advection of disturbance vorticity by the basic state thermal wind**.

Figure 9.3 displays the schematic structure of a baroclinic wave at 500 hPa (level 2 in the two layer model). Vertical motion is due to frontogenesis associated with the rotation of the isotherms. This rotation and the accompanying Q-vector is of opposite sign in the trough compared to in the ridge. In the trough the Q-vector points eastwards, while in the ridge it points westwards. This leads to Q-vector divergence to the west of the trough and Q-vector convergence to the east of the trough. Convergence of the Q_g-vector is associated with upward motion. The upward motion is observed to the east of the trough in the region of warm air advection. If the warm air travels upward and poleward, as shown by the solid arrow in **figure 9.4**, it replaces colder air. This is required for further growth of the wave. However, if warm air parcels travel poleward and upward, as shown by the dashed arrow in **figure 9.4**, it replaces warmer air. This implies a cooling of the warm sector of the wave, which does not reduce the potential energy of the background state, and hence is not conducive for further growth of the amplitude of the baroclinic wave.

Another way of looking at the dynamics of this process is by assuming, as in eq. 9.23, that

$$\zeta_2 = C\exp\left[i\left(lx + my - \omega t\right)\right] \tag{9.45}$$

and substituting (9.45) assumption into eq. 9.44. We then find that the forcing of vertical motion by zonal advection of disturbance vorticity by the basic state thermal wind, U_T, is proportional to the zonal wavenumber, l. Therefore the trajectories in the meridional plane will steepen with increasing zonal wavenumber, or decreasing zonal wavelength. In other words short waves will not grow by conversion of potential energy of the background state into kinetic energy of the disturbance.

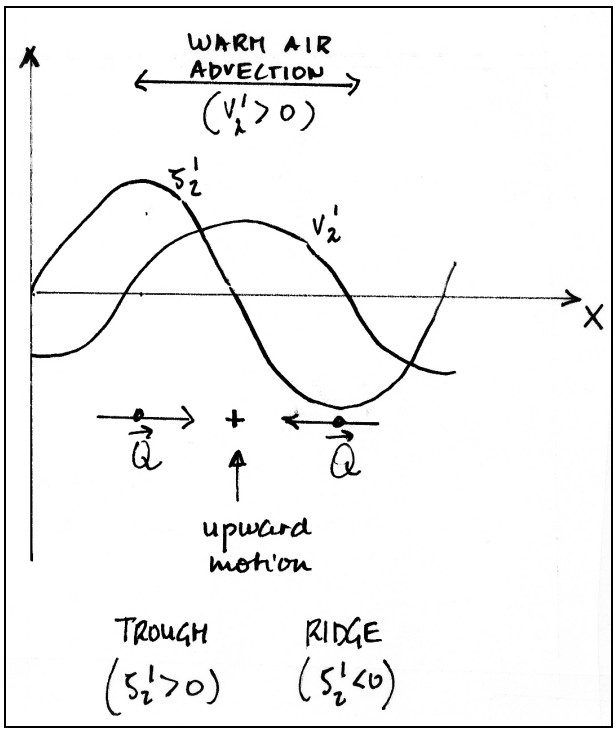

FIGURE 9.3. Structure of a baroclinic wave at midlevels (level 2 in the two-layer model, i.e. 500 hPa). The relative vorticity and the meridional velocity are shown as a function of longitude. The meridional velocity is 90° out of phase with the vorticity. See the text for further explanation.

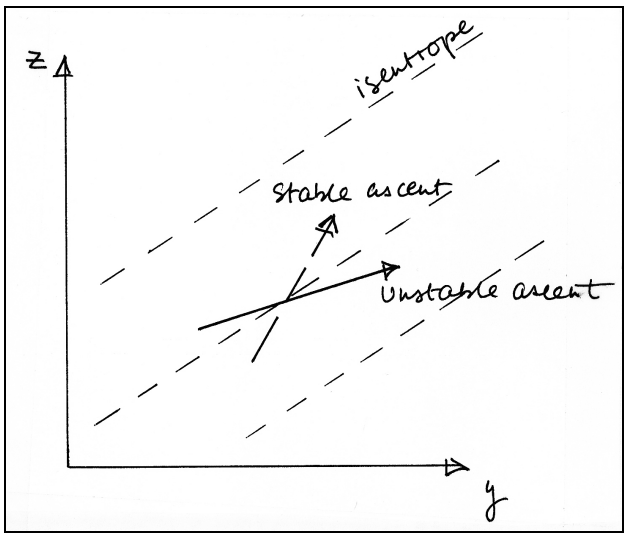

FIGURE 9.4. Illustration of mechanism of baroclinic instability (see text).

9.10 "PV-θ viewpoint" of forcing of vertical motion

Our qualitative knowledge of the characteristics of the solution of the PV-inversion equation for a steady PV-anomaly can provide illuminating insight into the relation between large-scale vertical motion and a **propagating PV-anomaly**. This is sometimes referred to as the "PV-θ viewpoint". Consider a positive potential vorticity anomaly embedded in a westerly mean flow with linear shear in height. The associated cyclonic circulation and the attraction of the isentropes towards the centre of the anomaly are sketched in **figure 9.5**. Let us assume that the PV-anomaly is located at a particular discrete height, it is represented mathematically by positive δ-function. If the coordinate system is such that the mean flow is zero at this level, then the circulation is a stationary solution of the equations of motion. Assuming adiabatic conditions, this implies that the isentropes do not move and that the air must flow among them. The air above the anomaly must flow down the isentrope to the west and up the isentrope to the east, as shown in **figure 9.5a**. Similarly, the air below the anomaly must flow up the isentropic surface to the east and down the isentropic surface to the west. Also, associated with the shear and thermal wind balance, isentropic surfaces must slope upwards towards the pole. Hence, as indicate in **figure 9.5a**, the poleward moving air to the east of the anomaly must ascend and the equatorward moving air to the west of the anomaly must descend. Therefore, the total **"isentropic upglide" vertical motion** is positive (ascent) to the east and negative (descent) to the west.

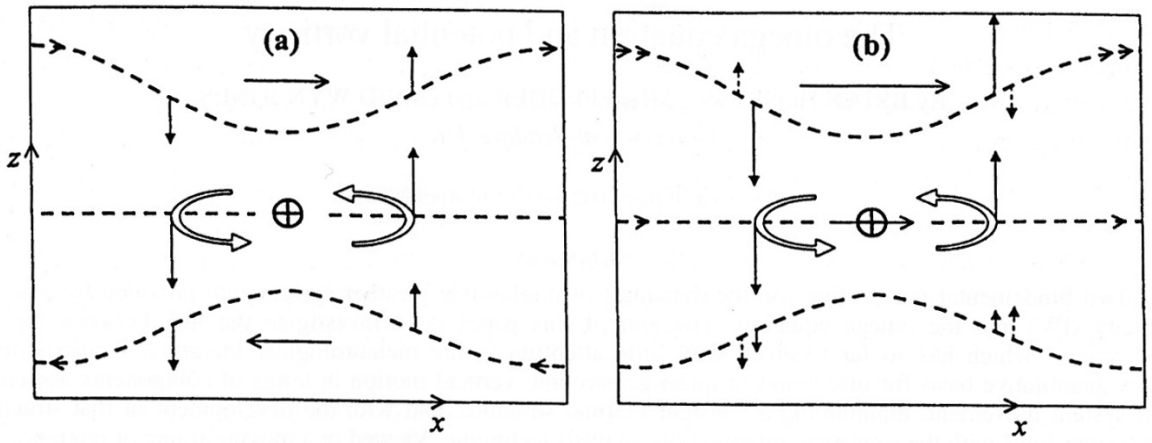

FIGURE 9.5. Schematic west-east vertical sections illustrating the effect of a positive potential vorticity δ-function superimposed on a westerly flow with a linear shear in height, z. Dashed lines represent isentropes. Horizontal and curved arrows sketch the horizontal circulation. Vertical pointing arrows indicate the vertical motion associated with isentropic upglide (continuous) and isentropic displacement (dashed). As viewed in a frame of reference in which (a) the anomaly appears stationary and (b) the zonal flow on the lower isentrope is zero, so that the anomaly appears to be moving from the left to the right (Hoskins, B.J., M. Pedder and D.W. Jones, 2003: The omega equation and potential vorticity. **Q.J.R.Meteorol.Soc**., 129, 3277-3303).

Suppose that the coordinate system is chosen such that the shear flow is zero in the neighbourhood of the lower isentrope (**figure 9.5b**). The components of the vertical motion associated with isentropic upglide in the meridional direction are unchanged. However, the westerly component now gives upglide vertical velocity at the lower isentrope, and larger values of isentropic upglide at the upper isentrope. Of course, the vertical motion is not dependent on the coordinate system. Therefore, there must be an additional part of the full

vertical motion associated with the translation of the potential vorticity anomaly in this coordinate system. We refer to this as the **"isentropic displacement" vertical motion**. As the PV-anomaly moves to the east the isentropes on the eastern side above the anomaly must move down and those below must move up (**figure 9.5b**). Similarly, on the western side the isentropes must return to their undisturbed level through ascent above and descent below. In this coordinate system it is the sum of the isentropic upglide and the isentropic displacement vertical motions that gives the same vertical motion as the isentropic upglide vertical motion in a frame of reference within which the translation of the anomaly appears stationary.

We have thus split the vertical motion into two components: the isentropic upglide associated with translation of air relative to PV-anomaly and the isentropic displacement associated with translation of a potential vorticity anomaly in a chosen reference frame and with its development (changing intensity). If the frame of reference is chosen such that the potential vorticity anomaly is stationary, the isentropic displacement vertical velocity is zero unless the potential vorticity anomaly is "developing" (changing intensity).

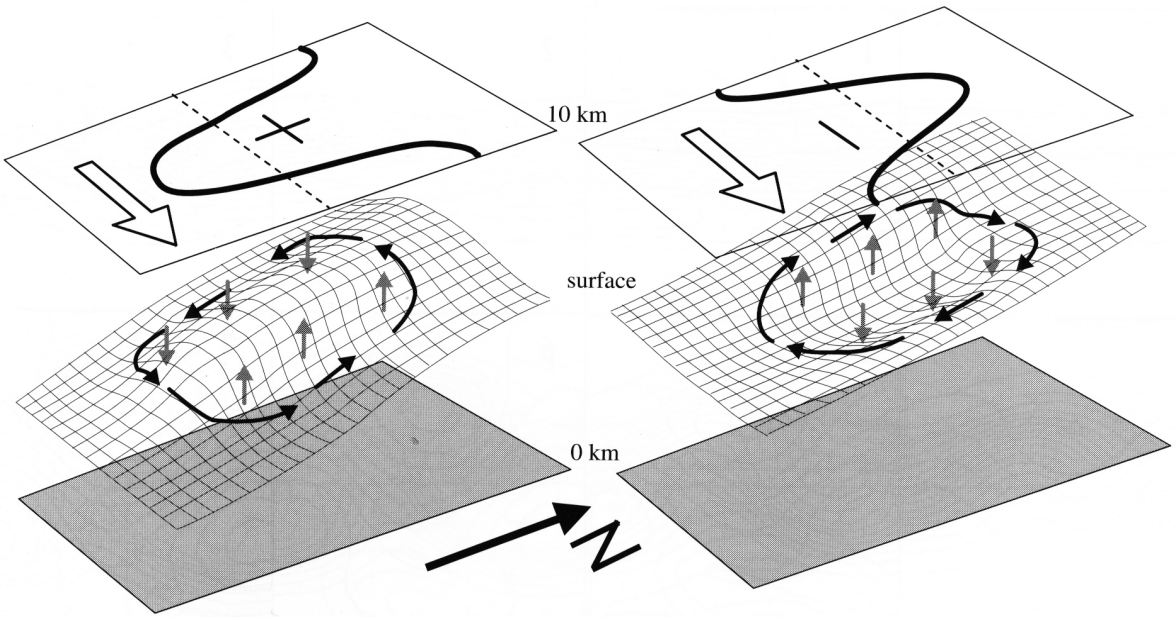

FIGURE 9.6. Topography of isentropic surfaces associated with eastward moving upper PV-anomalies. The dark lines mark the intersection of the tropopause with the 10 km level, separating air of PV> 2 PVU to the north from air of PV<2 PVU to the south. Shown also are system relative isentropic up-and downgliding (arrows directed along θ-surfaces) and vertical motion due to induced bulging of the isentropic surface (vertical arrows) when viewed from Earth-relative perspective. The dashed line represents a fixed latitude. Figure due to E.B. Carroll (published in **Meteorol.Apl.,** 10 (2003), p. 285.)

Figure 9.6 gives a three-dimensional view of what is meant by these concepts, where the potential vorticity anomaly pattern consists of a series of positive (associated with troughs in the northern hemisphere) and negative (associated with ridges in the northern hemisphere) anomalies embedded in a meridional potential vorticity gradient. The induced wind field is wavelike. There is upgliding meridional motion on the east side of the trough and downgliding meridional motion on the west side of the trough. The isentropic-displacement-component of the vertical motion is associated with the west-east (zonal) propagation of the series of troughs and ridges and depends on the phase speed of this wavelike pattern relative to the actual zonal velocity component of the air parcels.

Consider a frame of reference moving at some constant horizontal velocity (c_x, c_y). The potential temperature equation in this frame of reference is as follows.

$$\frac{d\theta}{dt} = \frac{\partial\theta}{\partial t} + (u - c_x)\frac{\partial\theta}{\partial x} + (v - c_y)\frac{\partial\theta}{\partial y} + w\frac{\partial\theta}{\partial z} = \frac{J}{\Pi} \qquad (9.46)$$

If this equation is divided by $\partial\theta/\partial z$ and taking into account that the slope of the isentrope in, for instance, the x-direction is

$$\frac{\partial z_\theta}{\partial x} = -\frac{\partial\theta/\partial x}{\partial\theta/\partial z} \qquad (9.47)$$

(z_θ is the height of the isentropic surface), the following equation for w is obtained.

$$w = \frac{\partial z_\theta}{\partial t} + (u - c_x)\frac{\partial z_\theta}{\partial x} + (v - c_y)\frac{\partial z_\theta}{\partial y} + \frac{J}{\Pi}\left(\frac{\partial\theta}{\partial z}\right)^{-1} \qquad (9.48)$$

The first term on the right hand side of eq. 9.48 is the **isentropic displacement vertical motion**. This term is interpreted physically as the "**the vaccuum cleaner effect**" of a PV-anomaly as follows. In adiabatic conditions, air rises in advance of an approaching upper level positive PV-anomaly, while air sinks in the lee of a retreating positive PV-anomaly. **Isentropic upglide/downglide vertical motion** (the second and third term in eq. 9.108) may, however, counter the vaccuum cleaner effect. The fourth term in eq. 9.48 represents the contribution of heating or cooling to vertical motion.

PROBLEM 9.1. **Maximum growthrate of a baroclinic disturbance** (taken from Holton, 2004).
Show, using eq. 9.29, that the maximum growth rate for baroclinic instability when β=0 occurs for

$$k^2 = 2\lambda^2(\sqrt{2} - 1) .$$

How long does it take the most rapid growing wave to amplify by a factor of e if $\lambda = 2\times10^{-6}$ m^{-1} and U_T=20 m s^{-1}.

PROBLEM 9.2. **Phase tilt of a baroclinic disturbance** (taken from Holton, 2004).
For the case β=0 determine the phase difference between the 250 hPa and the 750 hPa geopotential fields for the most unstable baroclinic wave (see problem 9.1).

ABSTRACT OF CHAPTER 9

Chapter 9 is concerned with the theory of mid-latitude baroclinic flow. The quasi-geostrophic approximation is used to formulate a **two-layer model** of the atmosphere in middle latitudes. The linear stability is analysed of a middle latitude zonal flow, in thermal wind balance, with a meridional temperature gradient, using the method of normal modes. The effect of the meridional variation of the Coriolis parameter (the **beta-effect**) is included. This analysis reveals the existence, in the two-level model, of so-called "**barotropic and baroclinic Rossby waves**". The amplitude of baroclinic Rossby waves grows exponentially in time if (1) **the vertical shear of the zonal wind exceeds a threshold value**, (2) **the zonal wavelength is larger than a critical value and**, (3) **the wave tilts westward with increasing height** (problem 9.7). The instability of baroclinic Rossby waves is invoked as a theory of **middle latitude cyclogenesis**.

The pattern of vertical motion in a baroclinic Rossby wave, with upward motion east of the trough and downward motion west of the trough, is understood from two perspectives: (1) the "**quasi-geostrophic viewpoint**" (omega equation and Q-vectors) and (2) the so-called "**PV-θ viewpoint**".

Further reading

Textbooks

Holton, J.R., 2004: **An Introduction to Dynamic Meteorology**. Academic Press, 529 pp. (chapter 6: quasi-geostrophic equations; chapter 8: two-level model and baroclinic instability)

Lackmann, G., 2011: **Midlatitude Synoptic Meteorology**. American Meteorological Society. 345 pp. (see chapter 3 on isentropic analysis and chapter 4 on potential vorticity).

Articles

Carroll, E.B., 2003: Thermal advection, vorticity advection and potential vorticity advection in extra-tropical synoptic-scale development. **Meteorol.Appl., 10**, 281-292. (Potential vorticity viewpoint of forcing of vertical motion**)**

Charney, J.G., 1949: On the physical basis for numerical prediction of large-scale motions in the atmosphere. **J.Meteorol., 6,** 372-385. (The original article on the quasi-geostrophic approximation)

Clough, S.A., C.S.A. Davitt and A.J. Thorpe, 1996: Attribution concepts applied to the omega equation. **Quart.J.Roy.Meteor.Soc**., **122**, 1943-1962. (An interesting paper that discusses the solution of the omega equation and the idea that frontogenesis induces circulations that "act at a distance", as was also shown in section 8.3 of these lecture notes)

van Delden, A., and R. Neggers, 2003: A case study of tropopause cyclogenesis. **Meteorol.Appl., 10**, 197-209**.** (Application of theoretical concepts introduced in this chapter to a case of cyclogenesis at the tropopause)

Hoskins, B., 1997: A potential vorticity view of synoptic development. **Meteorol.Appl., 4**, 325-334. (Explains the potential vorticity viewpoint of the development of large scale circulation systems with a minimum of mathematics: recommended literature)

Davies, H.C., 1997: Emergence of the mainstream cyclogenesis theories. **Meteorol.Zeitschrift**, N.F. **6**, 261-274. (This article gives an interesting account of the history of cyclogenesis theories)

Hoskins, B.J., I. Draghici and H.C. Davies, 1978: A new look at the omega-equation. **Quart.J.Roy.Meteor.Soc., 104**, 31-38. (The original paper that derived the most useful version of the omega equation, which shows the connection between frontogenesis and vertical motion)

Pedder, M.A., 1997: The omega equation: Q-G interpretations of simple circulation features. **Meteorol Appl., 4**, 335-344. (Compares different quasi-geostrophic versions of the omega equation: recommended literature)

Semple, A.T., 2003: A review and unification of conceptual models of cyclogenesis. **Meteorol.Appl**., **10**, 39-59.

List of problems (chapter 9)

This is the unchanged, but shortened version of the December 2015 version, of chapter 9 of the lecture notes on Atmospheric Dynamics (April 2020), written by Aarnout van Delden (IMAU, Utrecht University, Netherlands), a.j.vandelden@uu.nl .
http://www.staff.science.uu.nl/~delde102/AtmosphericDynamics.htm